Effect of Siloxane Segment Length on the Surface Composition of Poly(imidesiloxane) Copolymers and Its Role in Adhesion

Jin Zhao,[†,‡] Sergio R. Rojstaczer,[§] Jiaxing Chen,[†] Mingzhu Xu,[§] and Joseph A. Gardella, Jr.*[,†,||]

Department of Chemistry, State University of New York at Buffalo, Buffalo, New York 14260-3000, and Technology Center, Occidental Chemical Corporation, Grand Island, New York 14072

Received March 13, 1998; Revised Manuscript Received November 5, 1998

ABSTRACT: A series of poly(imidesiloxane) (SIM) copolymers, based on α,ω-aminopropylpoly(dimethylsiloxane) (PDMS), 2,2-bis(4-[4-aminophenoxyl]phenyl)propane (BAPP), and 4,4′-oxydiphthalic anhydride (ODPA) was synthesized in our laboratories. We investigated the effect of siloxane segment length on the surface composition of the SIM copolymers and its role in adhesion. The aim is to elucidate the correlation between polymer structure, surface composition, and adhesion strength. Composition−depth profiles of the near surface region to approximately 100 Å depth were calculated using an algorithm to numerically model and simulate the deconvolution of angle-dependent electron spectroscopy for chemical analysis (ESCA) experiments. The simulated composition−depth profiles show that the topmost surface of the air (free) surface of the 75 μm thick SIM copolymer film consists of a siloxane-rich layer, even with the shortest siloxane segment. For a given siloxane bulk content, a longer siloxane segment gives a surface richer in siloxane. The peel strength of these films from adhesion to a standard Fe/Ni alloy-42 decreases with increasing thickness of the surface siloxane-rich layer, which corresponds to a longer siloxane segment length. However, all values of peel strength of the SIM copolymers are higher than that of pure polyimide.

Introduction

Poly(imidesiloxane) (SIM) copolymers are becoming increasingly important materials in microelectronic applications,[1−17] such as die attach adhesives. Surface characterization of SIM copolymers has also been of interest in regard to applications involving adhesion to flexible semiconductors.[18] In recent years, the Occidental Chemical Corporation (OxyChem) has developed and commercialized a series of adhesives, based on SIM copolymers, for microelectronic applications. Work from our laboratories by Zhuang et al.[1] used ESCA to study the surface composition of a series of commercially available (OxySIM) SIM copolymers based on a proprietary mixed imide structure with different processing variations and different PDMS bulk content and segment length. They found that small amount of PDMS and short siloxane segments in the SIM copolymers yield a surface region with both PDMS and polyimide components. The adhesion strength of the SIM series was evaluated by peel tests on Fe/Ni Standard alloy-42 and correlated to the surface structure and bulk composition of the SIM copolymers. In particular, the highest adhesion strength comes from the SIM copolymer with only one dimethylsiloxane repeat unit. However, the detailed structure of the SIM copolymers studied was not divulged.[1] To quantitatively understand the effects of segment length and bulk composition on the surface composition and morphology of SIM copolymers, a study of a series of known structure SIM copolymers has been carried out in the present work.

In many phase-separated copolymer systems, the thermodynamic driving force for minimizing the total free energy of the system results in preferential surface segregation of the lower surface energy constituent. However, the extent and in-depth distribution of surface segregation in copolymers are affected by a number of other factors. These factors include bulk composition,[19,20] block length,[21,22] processing conditions (annealing,[19,20,22−24] casting solvent,[20,23,25] etc.) and block sequence distribution,[26] etc.

In a preliminary report[2] on the system under study, a series of poly(imidesiloxane) (SIM) copolymers, based on α,ω-aminopropylpoly(dimethylsiloxane) (PDMS), 2,2-bis-(4-[4-aminophenoxyl]phenyl)propane (BAPP), and 4,4′-oxydiphthalic anhydride (ODPA) was synthesized in our laboratories. The effects of siloxane segment length (average number of dimethylsiloxane repeat units = 1, 2, 3, 4, 5, and 9) and siloxane bulk content (1∼30 wt %) on the surface composition and morphology of the SIM copolymers were investigated. Angle-dependent ESCA measurements show that the dominant factor in defining the surface composition is not the bulk composition but instead the siloxane segment length. For a given PDMS bulk content, a longer siloxane segment gives a surface richer in PDMS, while for a given siloxane segment length, varying the PDMS bulk content does not significantly change the surface composition. Nevertheless, a full analysis of the effect of siloxane segment length on the composition−depth profile and its role in adhesion was not completed.

The measurement of in-depth profiles of composition near the surface of polymeric materials has drawn great interest in recent years. Ion beam sputter depth profiling has been used to extract composition−depth information on polymeric materials using detection by ESCA[14] and secondary ion mass spectrometry[27] (SIMS) experiments. Furukawa et al.[14] monitored the Si surface concentration of several poly(imidesiloxane) copolymers by ESCA experiment with Ar^+ sputtering. For the poly(imidesiloxane) copolymers with siloxane segment lengths

[†] State University of New York at Buffalo.
[‡] Current Address: Advanced Micro Devices, 5204 E. Ben White Blvd., Austin, TX 78741.
[§] Occidental Chemical Corporation.
[||] Electronic Address: gardella@acsu.buffalo.edu.

10.1021/ma980401n CCC: $18.00
Published on Web 01/08/1999

Scheme 1. Overall Scheme of Sample Preparation Process

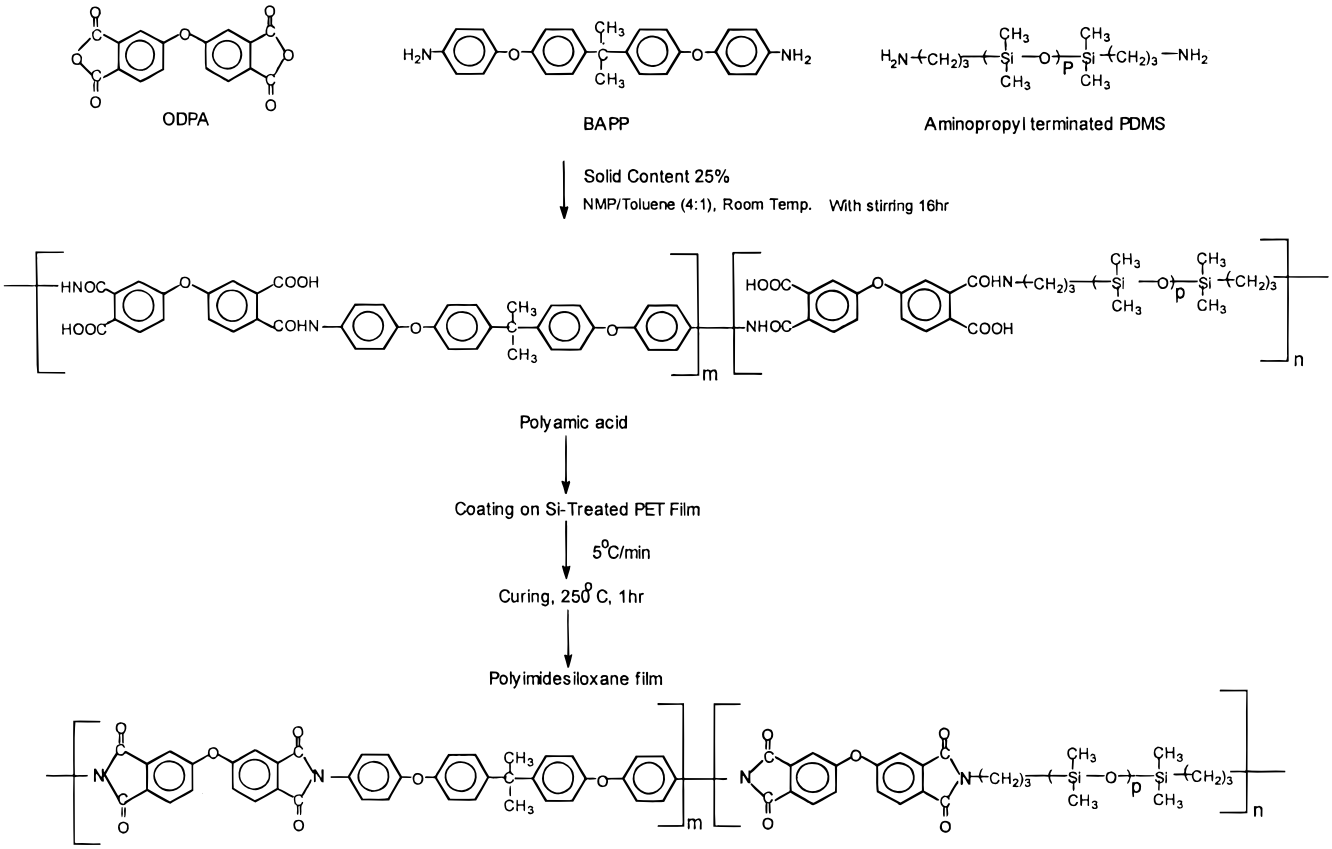

of 8 dimethylsiloxane repeat units, they estimated that the concentration gradient of Si is very high in the top surface of a thickness of 35−40 Å. After this region, the Si concentration decreases gradually with the sputtering time. Russell et al.[27] successfully characterized the composition−depth structure of polystyrene (PS)−poly(methyl methacrylate) (PMMA) copolymers (with either PS or PMMA being fully deuterated) by monitoring the $^2H^+$ and $^1H^+$ signals in the dynamic SIMS mode. However, the ion sputtering induced composition and morphology changes as well as the drawbacks related to ion sputtering, such as knock-on effects and ion-induced diffusion, are the major concerns with the accuracy of studying composition−depth profile of polymeric materials by ion sputtering methods. Other ion beam depth profiling methods, such as low energy ion scattering, Rutherford backscattering (RBS) and forward recoil, are used to study in depth distributions of polymers.[28] However, the depth resolution of these techniques is neither as good as ESCA nor is the region probed as shallow as that in ESCA.

Another category of experimental methods to extract composition−depth information of polymeric materials involves deconvolution of the experimental data. This category includes neutron reflection (NR)[29,30] and angle-dependent ESCA.[21,32−38] Experimentally varying the angle of the sample plane with respect to the analyzer yields different information depths (known as angle-dependent ESCA). However, the result from angle-dependent ESCA is not a direct in-depth profile of composition as a function of depth because all atoms within the path of the probing X-ray contribute to the signal but the contribution of each decreases exponentially with the distance from the free surface.[31] Similar to the neutron reflection experiment, deconvolution methods have been used to obtain the composition−depth profiles from the angle-dependent ESCA data. A major advantage of deconvolution of angle-dependent ESCA data lies in that it is nondestructive compared with the ion sputtering method. In the present work, a deconvolution program[21] was utilized to obtain composition−depth profiles from the angle-dependent ESCA results. This program assumes a model of surface segregation and boundary conditions based on the bulk composition. In particular, the effect of siloxane segment length (average number of dimethylsiloxane repeat units = 1, 2, 3, 4, 5, and 9) on the surface composition of the SIM copolymers with 10 wt % PDMS bulk content, a subset of the materials studied previously,[2] and its role in adhesion is presently investigated. The aim is to elucidate the correlation between polymer structure, surface composition, and adhesion strength. The adhesion strength was measured by peel test of SIM copolymers laminated on Fe/Ni alloy-42.

Experimental Section

Sample Preparation. The SIM copolymers for this study were prepared by the two-stage polyamic acid method. The overall scheme of sample preparation is shown in Scheme 1. First, α,ω-aminopropylpoly(dimethylsiloxane) (PDMS) (PCR, Inc.) was added, with stirring, to 2,2-bis(4-[4-aminophenoxyl]-phenyl)propane(BAPP) (WCK, Co.) in a combined solvent with a 4:1 mixture of 1-methyl-2-pyrrolidinone (NMP) and toluene. Then, 4,4′-oxydiphthalic anhydride (ODPA) (OxyChem, Co.) was added slowly, with stirring, to the above mixture. Different siloxane segment lengths in the SIM copolymers resulted from varying the p value in Scheme 1. Different copolymer bulk compositions (PDMS contents) resulted from varying the m/n ratio in Scheme 1. PDMS with average molecular weights (M_w) of 252, 334, 406, 475, 550 and 813 g/mol were used, corresponding to p = 1, 2, 3, 4, 5 and 9 in Scheme 1. The value of p

Table 1. N/Si and C/N Values of the Bulk Copolymers

	G-1−10	G-2−10	G-3−10	G-4−10	G-5−10	G-9−10
N/Si	3.67	3.16	2.86	2.60	2.45	2.14
C/N	18.09	18.75	18.92	19.09	19.52	20.09

Table 2. Glass Transition Temperature of the SIM Copolymers with Variation of Siloxane Segment Length for a Given 10 wt % PDMS Bulk Content

	G-1	G-2	G-3	G-4	G-5	G-9
T_g (°C)	165	170	178	171	190	210

represents an average segment length except for $p = 1$. In the present work, the PDMS content was kept constant at 10 wt %, and the different siloxane segment length was determined by the M_w of the siloxane−diamine monomer. The reaction mixture was stirred at room temperature for 16 h. The resulting polyamic acid solutions were drawn to silicone-treated PET film substrates with a doctor blade. The coated films were then placed in an oven at 70 °C and heated to 250 °C at a rate of 5 °C/min and then held at 250 °C for 60 min. The thickness of the imidized film was in the range of ∼60−90 μm. The air sides of the resulting thick films were analyzed by ESCA so as to determine the surface composition of the SIM copolymers. The specimens were denoted as G-*X*, where *X* represents the average siloxane segment length. The bulk N/Si and C/N values that were calculated from the starting materials are shown in Table 1.

ESCA. ESCA analysis was carried out in a Physical Electronic/PHI 5300 X-ray photoelectron spectrometer operated at 300 W (15 kV and 20 mA). Mg Kα radiation (1253.6 eV) and a pass energy of 89.45 eV for survey as well as 17.9 eV for high-resolution acquisition was used for all angle-dependent acquisitions. Binding energies were calibrated by setting C 1s at 285.0 eV. Photoelectron emission takeoff angles of 10, 20, 30, 45, and 90° were used for all samples. Signals from all four detectable elements (carbon, oxygen, nitrogen, and silicon) were recorded. For quantification, ESCA atomic sensitivity factors (ASF) relative to F 1s = 1.00 were used. The ASF applied are 0.27 for Si 2p, 0.42 for N 1s, 0.66 for O 1s and 0.25 for C 1s.[39,40] The concentration of each element was obtained from the ESCA signal area divided by the corresponding ASF.

Peel Test. The samples for the adhesion strength test are strips ($^1/_4$ in. × 1 in. or 6.3 mm × 25 mm) of the SIM copolymers. They were laminated onto Fe/Ni alloy-42 substrates at 350 ± 10 °C with 250lb pressure applied for 1 min. The Fe/Ni alloy-42 was ultrasonically cleaned with methylene dichloride three times. The peel tests were performed on a Diventro peel tester adapted with a 5 kg Omega digital force gauge connected to a strip chart recorder. The test was done in 90° geometry. The peel rate was 40 mm/min.

Table 2 shows the glass transition temperatures (T_g) of the SIM copolymers as a function of siloxane segment length at a constant 10 wt % siloxane bulk content. It is clear that the T_g of poly(imidesiloxane) copolymers increases with increasing siloxane segment length. This is consistent with our previous results.[41] This effect is likely due to the smaller extent of interphase mixing associated with the longer blocks of siloxane and polyimide segments.[42,43]

In general, the difference between the lamination temperature (T_1) of peel strength measurements and the glass transition temperature (T_g) of the copolymer is kept at a constant value and the best peel strength usually comes from a temperature range of $(T_1 - T_g) \cong 100-200$ °C. In our cases, SIM copolymer G-1 reached its highest adhesion strength at 350 °C, while other SIM copolymers, such as G-4, G-5, and G-9, flowed severely at lamination temperatures higher than 350 °C and resulted in poor peel strength. Considering the variation of the T_g of the SIM copolymers (Table 2), a constant lamination temperature of 350 °C, which is within the temperature range to obtain the best adhesion strength for all the SIM copolymers, was used in all the adhesion strength measurements.

Recovery of the Composition−Depth Profiles from Angle-Dependent ESCA Data. The principle of revealing the composition−depth profiles of the SIM copolymers is the same as that described in ref 21. The intensities of the photoelectronic response from carbon and nitrogen atoms as functions of the photoelectron takeoff angle can be formulated in the derivative as

$$dI_C(\theta) = F\alpha_C N_C(x) K e^{-x/(\lambda_C \sin\theta)}\, dx \quad (1)$$

$$dI_N(\theta) = F\alpha_N N_N(x) K e^{-x/(\lambda_N \sin\theta)}\, dx \quad (2)$$

where I is the detected intensity of photoelectrons from a given atom, subscripts C and N denote carbon and nitrogen, respectively, θ is the photoelectron takeoff angle, F is the X-ray flux, α is the cross-section of photoionization in a given shell of a given atom for a given X-ray energy, $N(x)$ is the depth profile of the atomic density, x is the vertical distance from the free surface, K is a spectrometer factor, and λ is the inelastic mean free path of the electrons. The inelastic mean free paths (IMFP) for C 1s and N 1s were calculated with the modified Bethe equation.[44] The resultant IMFPs of C 1s and N 1s electrons are about 18 and 17 Å, respectively, for all the synthesized SIM copolymers with an estimated density of 1.33 g/cm^3.

Assuming F, K, and α are independent of x and defining the normalized intensity $I'(\theta)$ as $I(\alpha)/(F\alpha K)$, one can integrate eqs 1 and 2 and obtain

$$I_C'(\theta) = I_C(\theta)/(F\alpha_C K) = \int_0^\infty N_C(x) e^{-x/(\lambda_C \sin\theta)}\, dx \quad (3)$$

$$I_N'(\theta) = I_N(\theta)/(F\alpha_N K) = \int_0^\infty N_N(x) e^{-x/(\lambda_N \sin\theta)}\, dx \quad (4)$$

or

$$I_C'(\theta)/I_N'(\theta) = [\int_0^\infty N_C(x) e^{-x/(\lambda_C \sin\theta)}\, dx]/[\int_0^\infty N_N(x) e^{-x/(\lambda_N \sin\theta)}\, dx] \quad (5)$$

Normalized intensities for different atoms at a photoelectron takeoff angle θ, usually reported as a ratio, such as I_C'/I_N', can be obtained from the ESCA data, as corrected by Vargo and Gardella.[40] In the present study, Table 3 gives the atomic ratio of I_C'/I_N' in the SIM copolymers obtained by angle-dependent ESCA experiments.

In the previous work using this deconvolution method,[21] the poly(dimethylsiloxane-urethane) (PDMS−PU) segmented copolymer chains are divided into PDMS soft segments and PU hard segments. Since nitrogen is unique to the PU hard segments, the weight percentage of PDMS (soft segment) or PU (hard segment) can be calculated from the atomic ratio of carbon to nitrogen (C/N). The reason for using the ratio of photoelectron intensities of carbon to nitrogen to calculate the PDMS surface concentration is due to the relatively large variation in nitrogen signal at different photoelectron takeoff angle, while the variation of silicon signal is within the experimental error. In the present work, the SIM copolymer chains are similarly divided into siloxane soft segments and polyimide hard segments. Assuming that changes in density throughout the film (<5%) and the difference between weight fraction and volume fraction values (<3%) are negligible and given that $v(x)$ is the depth profile of the polyimide hard segments, the atomic depth profiles for carbon and nitrogen are

$$N_C(x) = \eta v(x) + \sigma(1 - v(x)) \quad (6)$$

$$N_N(x) = \eta v(x)\gamma \quad (7)$$

The weight fraction (C) of polyimide hard segments, the number density (η) of carbon atoms in the polyimide hard

Table 3. Atomic Ratio of I_C'/I_N' in the Poly(imidesiloxane) (±5%), Determined by Angle-Dependent ESCA As Reflected by Peak Ratios Prior to Deconvolution

take-off angle (deg)	G-1−10	G-2−10	G-3−10	G-4−10	G-5−10	G-9−10
10	30.5 ± 1.5	36.9 ± 1.8	43.0 ± 2.2	50.5 ± 2.5	58.4 ± 2.9	64.6 ± 3.2
30	23.9 ± 1.2	25.8 ± 1.3	27.7 ± 1.4	30.0 ± 1.5	31.2 ± 1.6	33.9 ± 1.7
45	19.9 ± 1.0	21.8 ± 1.1	23.9 ± 1.2	24.8 ± 1.2	24.3 ± 1.2	25.8 ± 1.3
90	19.1 ± 1.0	21.0 ± 1.1	21.6 ± 1.1	22.0 ± 1.1	23.1 ± 1.2	25.5 ± 1.3

Table 4. Parameters Used in Recovering the Composition−Depth Profiles

	G-1	G-2	G-3	G-4	G-5	G-9
C	0.90	0.90	0.90	0.90	0.90	0.90
η	61.90	62.22	62.43	62.58	62.69	62.93
σ	46.30	41.38	38.46	36.53	35.16	32.18
γ	0.0560	0.0536	0.0523	0.0515	0.0508	0.0494

segments, the number density (σ) of carbon atoms in the siloxane soft segments, and the atomic ratio (γ) of N/C in polyimide hard segments for different SIM copolymers were calculated and summarized in Table 4.

A Gaussian distribution model with four-parameters was constructed to simulate the volume fraction $v(x)$ of polyimide hard segments

$$v(x) = CH \exp[-0.5(x - L)^2/S_1^2] \quad x \le L$$

$$= C\{1 + (H - 1) \exp[-0.5(x - L)^2/S_2^2]\} \quad x > L \qquad (8)$$

where H is a parameter relevant to the magnitude of the trough in the profile, x is the distance from the free surface (in Å), L is the location of the trough in the profile, S_1 characterizes the shape of the profile to the left of the trough, S_2 characterizes the shape of the profile to the right of the trough, and C is the volume fraction of polyimide hard segments in the bulk (again, assuming the difference between weight fraction and volume fraction values is negligible).

The ratio of the intensities of photoelectrons from carbon and nitrogen, designated as R, can be calculated using eq 5 by inserting eqs 6−8 and adjusting the four parameters in eq 8. This result is then compared with the data from angle-dependent ESCA experiments. To reach the optimal values of these four parameters, the following objective function was used:

$$\psi = \{(1/n)\sum^{n}[[R_{cal}(H,L,S_1S_2) - R_{exp}(\theta_n)]/R_{exp}(\theta_n)]^2\}^{1/2} \qquad (9)$$

Here n is the number of photoelectron takeoff angles (n is equal to four in the present study). The optimization was achieved using the algorithm developed by Dr. Tai Ho[21] and programmed in Mathcad 5.0 (MathSoft, Inc.). Using this algorithm, the four parameters (H, L, S_1, S_2) in eq 8 were adjusted to calculate the volume fraction depth profile of the polyimide hard segments − $v(x)$, which was then inserted into eqs 6 and 7. The calculated atomic depth profiles of carbon ($N_C(x)$) and nitrogen ($N_N(x)$) were put into eq 5 to calculate the R_{cal} which is defined as $I_C'(\theta)/I_N'(\theta)$. The calculated R_{cal} and the experimental R_{exp} (Table 3) were inserted into the objective eq 9. Through adjusting the four parameters (H, L, S_1, S_2) in eq 8, the optimal value of ψ was reached. The adjusted four parameters (H, L, S_1, S_2) were inserted back to eq 8 to calculate the volume fraction depth profile of the polyimide hard segments − $v(x)$, which represents the surface composition of the SIM copolymers. For each sample of a particular segment length at constant 10 wt % bulk content, four replicates of angle-dependent ESCA analysis were averaged at each angle to obtain $R_{exp}(\theta)$. Error estimates leading to error bars are the result of the variance from the fitting of the optimum objective functions (eq 9).

Results and Discussion

Surface Composition. As noted in the Introduction, the preliminary ESCA analysis[2] of a large set of samples ranging from 1 to 30 wt % PDMS and varying segment lengths (average number of dimethylsiloxane repeat units =1, 2, 3, 4, 5, 9) yielded the result that all polymers with the same PDMS segment length, but different siloxane bulk composition, give equivalent angle-dependent ESCA profiles save the 1% samples. The latter were noted to have a PDMS concentration too low for all chains to include PDMS. The factor that governed changes in ESCA angle-dependent profiles, including segmental differences in topmost surface composition, was the segment length of the PDMS. For the present study on the relationship of the in-depth profile and peel strength, we chose a subset of the composition range at 10 wt % with varying segment lengths. We note that typical composition of the commercial OxySIM polymers range from 2 to 15 wt %, so this composition was a representative of those materials.

Parts a and b of Figure 1 show the high-resolution ESCA spectra of C 1s at various photoelectron takeoff angles, as exemplified by samples SIM G-1−10 and G-9−10. The small peak at around 288.5 eV is attributed to −C(═O)−N−, which is characteristic of polyimide. In both parts a and b of Figure 1, the intensity of this peak increases progressively with increasing photoelectron takeoff angle. This suggests that the concentration of polyimide is lower at the topmost surface than in the deeper surface, while the concentration of PDMS exhibits the opposite trend. Furthermore, it is noticed that the intensity of this −C(═O)−N− peak increases sharply at photoelectron takeoff angle of 10−20° for sample G-1−10, while this variation happens at photoelectron takeoff angle of 20−30° for sample G-9−10. This means that the polyimide concentration of G-1−10 with depth increases faster than that of G-9−10 does. In other words, there are more PDMS at the sample surface of G-9−10 than that of G-1−10. However, these results from angle-dependent ESCA do not form a direct in-depth profile of composition as a function of depth because all atoms within the path of the probing X-ray contribute to the signal, but the contribution of each decreases exponentially with the distance from the free surface.[31]

Figure 2 shows the composition−depth profiles for the siloxane component in each copolymer recovered from the angle-dependent ESCA data, utilizing the deconvolution method described above. These composition−depth profiles reveal some features that are not obvious in the raw ESCA data. First, it is clear that siloxane was segregated to the sample surface forming a topmost siloxane-rich layer. This topmost siloxane-rich layer is followed by a siloxane depletion region. This is an inherent result of the assumed boundary conditions. It is assumed that any surface excess layer of the siloxane segment must necessarily be balanced by a siloxane depletion layer, because the average composition of the siloxane segment integrated over one polymer chain length must be equal to its bulk composition.[21] Scheme 2 shows the proposed surface structure of the backbone of the SIM copolymers. It demonstrates the siloxane-

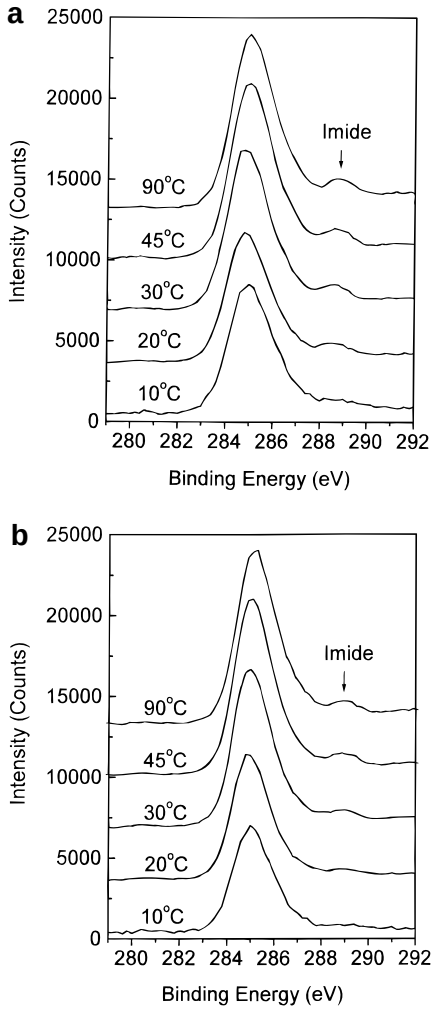

Figure 1. High-resolution ESCA spectra of C 1s at photoelectron takeoff angle of 10, 20, 30, 45, and 90°, as exemplified by sample SIM G-1−10. (b) High-resolution ESCA spectra of C 1s at photoelectron takeoff angle of 10, 20, 30, 45, and 90°, as exemplified by sample SIM G-9−10.

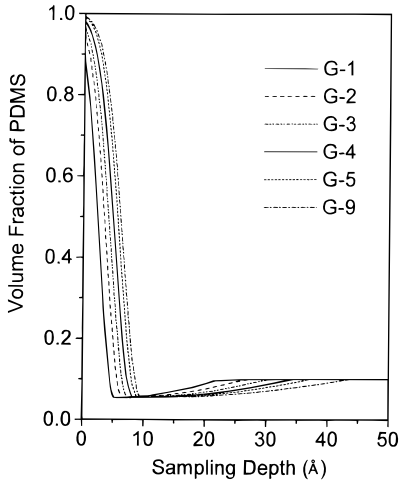

Figure 2. Deconvoluted concentration-depth profile with variation of the average PDMS segment length.

rich region and siloxane depletion region, though the real surface consists of all the statistically possible surface configurations of the backbone of SIM copolymers.

This analysis allows a way to extrapolate the surface composition at zero sampling depth from these profiles.

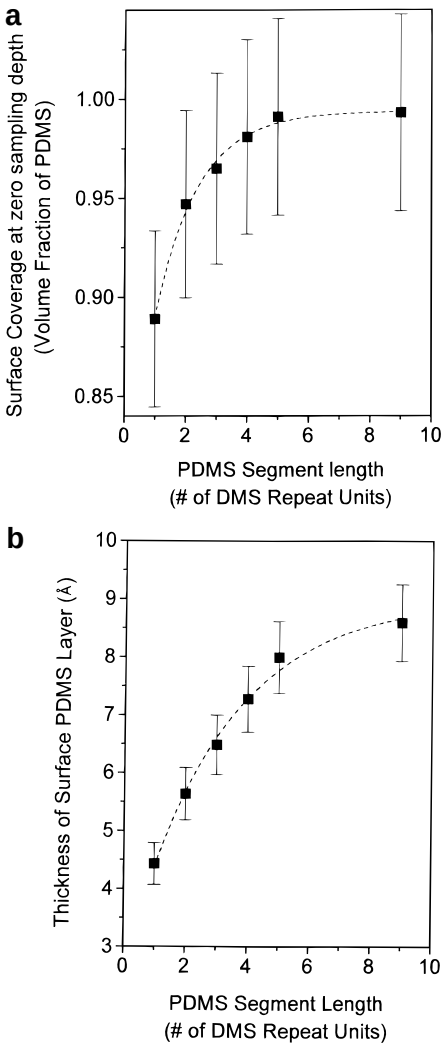

Figure 3. (a) Correlation between the PDMS surface coverage at zero sampling depth and the average PDMS segment length in the SIM copolymers. (b) Correlation between the thickness of surface PDMS-rich layer of SIM copolymers and the average PDMS segment length in the SIM copolymers.

Scheme 2. Proposed Surface Structure of the Backbone of the SIM Copolymers

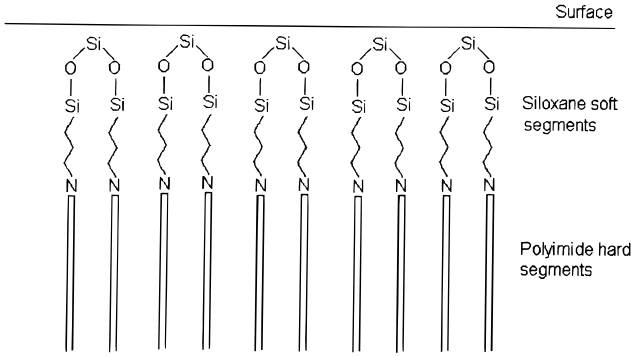

Figure 3a shows the volume fractions of siloxane component at the very top surface (sampling depth equal to zero) for these SIM copolymers. With the same 10 wt % PDMS bulk content, the very top PDMS surface coverage varies from 0.889 to 0.993 with an increase in the siloxane segment length, and dimethylsiloxane repeat units are equal to 1, 2, 3, 4, and 5−9. The very top PDMS surface coverage increases with increasing siloxane segment length. This suggests that only a small

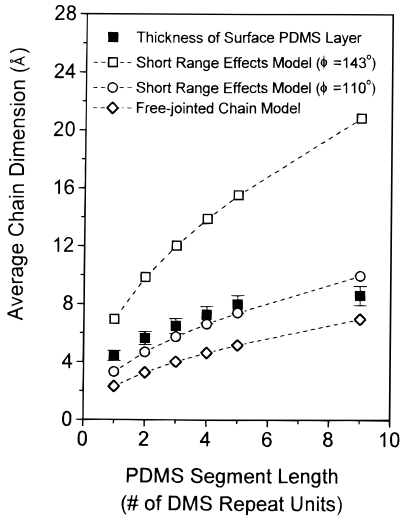

Figure 4. Correlation between the thickness of surface PDMS-rich layer of SIM copolymers and the calculated PDMS chain dimensions.

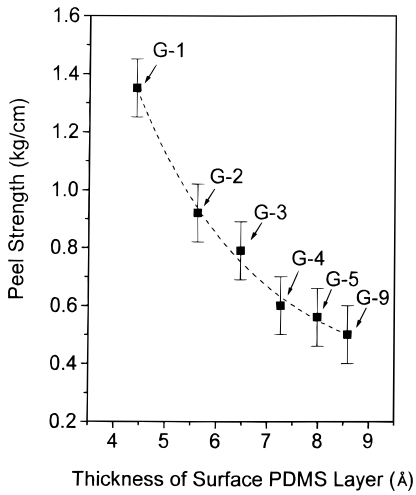

Figure 5. Correlation between the adhesion strength of SIM copolymers and the thickness of surface PDMS-rich layer from deconvoluted ESCA data.

amount of polyimide component or no polyimide component exists at zero sampling depth of these SIM copolymers.

Of particular interest is the thickness of the siloxane-rich layer defined as the depth from the very top surface to where the PDMS volume fraction reaches its bulk content. Figure 3b shows the thickness of the siloxane-rich layer with variation of siloxane segment length. With the same 10 wt % PDMS bulk content, varying the siloxane segment length, dimethylsiloxane repeat units equal to 1, 2, 3, 4, and 5−9, gives thicknesses (±5%) of the surface siloxane-rich layer of 4.4, 5.6, 6.5, 7.3, 8.0, and 8.6 Å, respectively. This is to say that, for a given PDMS bulk content in the SIM copolymers, a longer siloxane segment gives a thicker siloxane-rich layer at the sample surface. The thickness of the surface siloxane-rich layer also increases with increasing of the siloxane segment length.

The thickness of surface siloxane-rich layer recovered from the deconvoluted composition−depth profiles is comparable with the chain dimensions of the siloxane segments. Figure 4 shows the comparison of the thickness of surface siloxane-rich layer and the average chain dimensions of siloxane segment calculated from a free-jointed chain model and also a short-range effects model.[42] A bond length of Si−O in PDMS of 1.64 Å[46,47] was used in the calculation. To simplify the calculation, the chain dimension values of the siloxane segments from the short-range effects model were calculated using either the bond angle of Si−O−Si in PDMS of ∼143° or the bond angle of O−Si−O in PDMS of ∼110°.[46,47] The real values of the chain dimensions of the siloxane segments from the short-range effects model must be between the above two calculated values. When the siloxane segment length equals 1 or 2 dimethylsiloxane units, the thickness of the surface siloxane-rich layer is between the chain dimension values calculated by the free-jointed chain model and the short-range effects model. This is because the expansion of a polymer chain is restricted by the bond angles between each chain atom.[46] The short-range effects become more significant toward shorter chains, though the short range effects model may not be appropriate with extremely short siloxane segments such as dimethylsiloxane repeat units equal to 1 or 2. With increasing siloxane segment length, the PDMS chain gets more freedom, especially[46] with a Si−O bond length of 1.64 Å, which is significant longer than that of C−C bond (1.53 Å) of the general polymer skeletal bond and the Si−O−Si bond angle of ∼143° which is more open than the usual tetrahedral bond angle of ∼109°. This is the confirmation that, with increasing siloxane segment length, the thickness of surface siloxane-rich layer approaches the chain dimension value calculated by the free-jointed chain model.

Adhesion Strength. The adhesion strength measured by peel test of SIM copolymers laminated to Fe/Ni alloy-42 was plotted against the recovered thickness of surface siloxane-rich layer in Figure 5. It shows that the peel strength, ranging from 1.35 kg/cm of G-1 to 0.50 kg/cm of G-9, decreases with increasing of the thickness of surface siloxane-rich layer, though the peel strengths of all SIM copolymers are greater than that of pure polyimide polymer (0.25 kg/cm). This is evidence that both PDMS and polyimide are essential components to rendering high peel strength. To achieve high adhesion strength, there must be a component in the adhesive that presumably interacts with the substrate through strong chemical interactions (e.g., polyimide). However, it is equally important to have sufficient diffusive ability or ductility for the adhesive to achieve intimate contact with substrate.[48] PDMS has a good diffusive ability and readily reaches the substrate upon being pressed, so as to achieve intimate contacts. Imide groups interact with the substrate presumably through strong chemical interactions, so as to achieve adhesion. A longer siloxane segment in the SIM copolymers hinders the efficacy of adhesion due to a thicker siloxane-rich surface layer. This hindrance effect increases with increasing of the thickness of the surface siloxane-rich layer, which is determined by the siloxane segment length in the SIM copolymers. In our previous work,[1] surface composition of SIM sample side (OxyChem), after bonding to Fe/Ni alloy-42 and peeling off, and that of polymer-contacting side of alloy-42 after peeling were studied by angle-dependent ESCA. It is found that the nitrogen content in the top surface of the film after bonding raised ∼4-fold and the silicon content dropped by ∼4-fold, compared with the surface composition of the film prior to bonding. In the meantime, a significant amount of the imide portion of the SIM copolymer was observed by detecting nitrogen on alloy-42 after peeling. This indi-

cates that a cohesive failure is involved and that metal-imide interactions may be involved in the adhesive interaction. Nevertheless, it is worth further study to systematically evaluate the interaction mechanism and failure mechanism involved in bonding the SIM copolymers of different siloxane segment lengths to Fe/Ni alloy-42.

Conclusions

We investigated the effect of siloxane segment length on the surface composition of the SIM copolymers and its role in adhesion with the aim to elucidate the correlation between polymer structure, surface composition, and adhesion strength. Composition−depth profiles of the near surface region to approximately 100 Å depth were simulated from the angle-dependent ESCA results. The simulated composition−depth profiles show that the topmost surface of the air (free) surface of the ca. 75 μm thick SIM film was covered by a siloxane-rich layer, even with the shortest siloxane segment. Both the very top PDMS surface coverage (sampling depth equal to zero) and the thickness of the surface siloxane-rich layer increase with increasing of the siloxane segment length in the SIM copolymers. The adhesion strength measured by peel strength testing of SIM copolymers laminated to Fe/Ni alloy-42 decreases with increasing of the thickness of the surface siloxane-rich layer, corresponding to longer siloxane segment length, though all values of the adhesion strength of SIM copolymers are higher than that of pure polyimide. This confirms our previous results that both PDMS and polyimide are essential components to rendering high adhesion strength. PDMS component provides a good diffusive ability, while imide component interacts with the substrate to give rise to adhesion strength. A longer siloxane segment in the SIM copolymers hinders the efficacy of adhesion due to a thicker siloxane-rich surface layer.

Acknowledgment. J.Z. and J.A.G. acknowledge support from the Office of Naval Research.

References and Notes

(1) Zhuang, H. Z.; Gardella, J. A., Jr.; Incavo, J. A.; Rojstaczer, S. R.; Rosenfeld, J. C. *J. Adhes.* **1997**, *63*, 199.
(2) Zhao, J.; Rojastaczer, S. R.; Gardella Jr., J. A. *J. Vac. Sci. Technol. A* **1998**, *16*, 3046.
(3) Kuckertz, V. H. *Macromol. Chem.* **1996**, *4−5*, 212.
(4) Dwight, D.; McGrath, J. E.; Lawson, G.; Patel, N.; York, G. *Contemp. Top. Polym. Sci.* **1989**, *6*, 265.
(5) Yoon, T. H.; Arnold-McKenna, C. A.; McGrath, J. E. *J. Adhes.* **1992**, *39*, 15.
(6) William, M. C.; Spontak, R. *Polym. J.* **1988**, *20*, 649.
(7) William, M. C.; Spontak, R. *J. Appl. Polym. Sci.* **1989**, *38*, 1607.
(8) Cho, K.; Lee, D.; Seo, K. H.; Ahn, T. O. *ANTEC* **1995**, 2889.
(9) Berger, A. U.S. Pat. 4,395,527, 1983.
(10) Lee, C. J. U.S. Pat. 4,670,497, 1987.
(11) Rojstaczer, S. R. U.S. Pat. 5,209,981.
(12) Rojstaczer, S. R.; Tang, D. Y.; Tyrell, J. A. U.S. Pat. 5,317,-049.
(13) Keohan, F. L.; Hallgren, J. E. In *Silicon-Based Polymer Science: A Comprehensive Resource*, Zeigler, J. M., Ed.; American Chemical Society: Washington, DC, 1990; p 165.
(14) Furukawa, N.; Tamada, Y.; Furukawa, M.; Yuasa, M.; Kimura, Y. *J. Polym. Sci., Part A: Polym. Chem.* **1997**, *35*, 2239.
(15) Yamada, Y.; Furukawa, N. *Polym. J.* **1997**, *29*, 923.
(16) Hedrick, J. L.; Brown, H. R.; Volksen, W.; Sanchez, M.; Plummer, C. J. G.; Hilborn, J. G. *Polymer* **1997**, *38*, 605.
(17) Volksen, W.; Hedrick, J. L.; Russell, T. P.; Swanson, S. *J. Appl. Polym. Sci.* **1997**, *66*, 199.
(18) Na, M. H.; Haetty, J.; Zhao, J.; Chang, H. C.; Lee, E. H.; Luo, H.; Petrou, A.; Gardella, J. A., Jr. *Proceedings of Fourth International Conference on Frontiers of Polymers and Advanced Materials*; Cairo, Egypt, January, 1997.
(19) Chen, X.; Lee, H. F.; Gardella, J. A., Jr. *Macromolecules* **1993**, *26*, 4601.
(20) Chen, X.; Gardella, J. A., Jr.; Cohen, R. E. *Macromolecules* **1994**, *27*, 2206.
(21) Chen, X.; Gardella, J. A., Jr.; Ho, T.; Wynne, K. J. *Macromolecules* **1995**, *28*, 1635.
(22) Chen, X.; Gardella, J. A., Jr.; Kumler, P. L. *Macromolecules* **1993**, *26*, 3778.
(23) Zhuang, H. Z.; Gardella, J. A., Jr. *Macromolecules* **1997**, *30*, 3632.
(24) Coulon, G.; Russell, T. R.; Deline, V. R.; Green, P. F. *Macromolecules* **1989**, *22*, 2581.
(25) Thomas, T. R.; O'Malley, J. J. *Macromolecules* **1979**, *12*, 323.
(26) Li, L.; Chan, C. M.; Weng, L. T. *Macromolecules* **1997**, *30*, 3698.
(27) Russell, T. P.; Deline V. R.; Wakharkar, V. S.; Coulon, G. *MRS Bull.* **1989**, *10*, 33.
(28) Kramer, E. J., *MRS Bull.* **1996**, *17*, 37.
(29) Kramer, E. J.; Jones, R. A. L.; Norton, L. J. *Polym. Prepr. Polym. Chem. Am. Chem. Soc. (Div.)* **1990**, *21* (2), 75.
(30) Genzer, J.; Faldi, A.; Oslanec, R.; Composto, R. J. *Macromolecules* **1996**, *29*, 5438.
(31) Clark, D. T. *Adv. Polym. Sci.* **1977**, *24*, 126.
(32) Zhuang, H. Z.; Marra, K. G.; Ho, T.; Chapman, T. M.; Gardella, J. A., Jr. *Macromolecules* **1996**, *29*, 1660.
(33) Pijolat, M.; Hollinger, G. *Surf. Sci.* **1977**, *24*, 126.
(34) Iwasaki, H.; Nishitani, R.; Nakamura, S. *Jpn. J. Appl. Phys.* **1978**, *17*, 1519.
(35) Holloway, P. H.; Bussing, T. D. *Surf. Interface Anal.* **1992**, *18*, 251.
(36) Nefedov, V. I.; Baschenko, O. A. *J. Electron Spectrosc. Relat. Phenom.* **1988**, *47*, 1.
(37) Tyler, B. J.; Castner, D. G.; Ratner, B. D. *Surf. Interface Anal.* **1989**, *14*, 443.
(38) Jisl, R. *Surf. Interface Anal.* **1990**, *15*, 719.
(39) *Handbook of X-ray Photoelectron Spectroscopy*, Perkin-Elmer Corporation: Norwalk, CT, 1979.
(40) Vargo, T. G.; Gardella, J. A., Jr. *J. Vac. Sci. Technol.* **1989**, *A7*, 1733.
(41) Rojstaczer, S. R.; Tyrell, J. A.; Tang, D. Y. Unpublished results.
(42) Clarson, S. J. In *Siloxane Polymers*; Clarson, S. J., Ed.; PTR Prentice Hall, Inc.: Englewood Cliffs, NJ, 1993; p 218.
(43) Kennan, J. J. In *Siloxane Polymers*; Clarson, S. J., Ed.; PTR Prentice Hall, Inc.: Englewood Cliffs, NJ, 1993; p 108.
(44) Tanuma, S.; Powell, C. J.; Penn, D. R. *Surf. Interface Anal.* **1993**, *21*, 165.
(45) Cowie, J. M. G. *Polymers: Chemistry & Physics of Modern Materials*, 2nd ed.; Blackie and Son Limited: Glasgow, Scotland, 1991; p 215.
(46) Mark, J. E. In *Silicon-Based Polymer Science: A Comprehensive Resource*; Zeigler, J. M., Ed.; American Chemical Society: Washington, DC, 1990; p 47.
(47) Owen, M. J. In *Siloxane Polymers*; Clarson, S. J., Ed.; PTR Prentice Hall, Inc.: Englewood Cliffs, NJ, 1993; p 333.
(48) Wu, S. *Polymer Interface and Adhesion*; Marcel Dekker: New York and Basel, p 337.

MA980401N